RADIATIVE HEATING IN THE TROPOSPHERE AND LOWER STRATOSPHERE [1]

G. M. JURICA

Institute of Atmospheric Physics, The University of Arizona, Tucson, Ariz.

ABSTRACT

Brooks' method for computing rates of atmospheric heating which is due to radiation by water vapor has been adapted to the digital computer, allowing investigation of the following aspects of the method: the effect of spacing of data points on heating rate profiles, the dependence of heating rates upon the flux emissivity data, and the influence of the form of the pressure correction factor upon heating rates. Two cases of practical interest have been considered. The first is the effect of radiative heating upon tropospheric temperature inversions. It is concluded, in agreement with the results of Staley, that radiative heating acts to strengthen the inversion when water vapor mixing ratios within the inversion layer are small. The second case studied the consequences of the presence of substantial quantities of water vapor in the stratosphere. Cooling rates ranging up to 2.5° C. day^{-1} were obtained over a winter cross section of the Northern Hemisphere having a constant relative humidity of 5 percent in the stratosphere. Decreases in the net radiative flux, as evidenced by small heating rates in the region of the tropopause at low latitudes, agree with observations by Riehl in the Caribbean and by Kuhn and Suomi in the United States. The fact that this effect was not present when mixing ratios were allowed to decrease rapidly above the tropopause lends support to the argument that substantial quantities of water vapor are present in the stratosphere.

1. INTRODUCTION

The importance of the role played by radiative cooling to the dynamics of the atmosphere has long been recognized. As a result, considerable effort has been devoted to computing the rate of radiative temperature change in the free atmosphere from radiosonde data. Predominant among these efforts are a variety of radiation charts produced by Mügge and Möller [10], Elsasser [4], Möller [9], Robinson [12], and Yamamoto and Onishi [15]. However, it was Bruinenberg [3] who first emphasized two important points: the superiority of numerical methods over graphical techniques for this problem, and the advantage of calculating radiative temperature changes directly from a flux divergence equation rather than from finite differences of fluxes. Brooks [1] modified Bruinenberg's original equation and presented his form of the equation for radiative temperature change

$$\frac{\partial T}{\partial t}=\frac{g}{c_p}\left(\frac{p}{1000}\right)^{1/2}\left\{\sum_{n=1}^{N}\Delta(\sigma T^4)_n\left(\overline{\frac{\partial\epsilon(kw,\,T)}{\partial w}}\right)_n+\left(\sigma T^4\,\frac{\partial\epsilon(kw,\,T)}{\partial w}\right)_{w_T}-\sum_{m=1}^{M}\Delta(\sigma T^4)_m\left(\overline{\frac{\partial\epsilon(kw,\,T)}{\partial w}}\right)_m\right\} \tag{1}$$

In equation (1) T is absolute temperature, q is the specific humidity of water vapor, c_p is the specific heat of air at constant pressure, σ is the Stefan-Boltzmann constant, ϵ is flux emissivity, k is the absorption coefficient, and w is the corrected optical thickness of water vapor. The quantity $(p/1000)^{1/2}$ is a pressure correction factor to give the corrected optical thickness of water vapor within a given layer having a mean pressure p. The summation over n is for the N layers above the reference level for which $\partial T/\partial t$ is being calculated, and the summation over m is for the M layers between the reference level and the ground. The term $[\sigma T^4\partial\epsilon(kw,\,T)/\partial w]_{w_T}$ is to be evaluated at the top of the water vapor atmosphere, where the optical distance from the reference level is $_{w_T}$. For an atmosphere in which temperature decreases with height, the first and second terms in equation (1) contribute to cooling while the third term contributes to warming at the reference level.

The details of the calculation of radiative heating rates are explained in Brooks' [1] paper; however, for convenience a brief description will be presented here. Radiosonde data are obtained and the atmosphere is divided into a number of layers, the boundaries of the layers ordinarily being chosen at the significant levels of the sounding. The value of $\Delta(\sigma T^4)$, the corrected thickness of water vapor, and the value of $\overline{\partial\epsilon(kw,\,T)/\partial w}$ in each layer are then calculated. Proper insertion of these values into equation (1) yields the heating rate at the reference level.

Although straightforward, this procedure becomes prohibitively time-consuming for the person wishing to make detailed analyses or to investigate the behavior of Brooks' method. Therefore, the method was adapted to a digital computer program which duplicates exactly the procedure described by Brooks with the following exception. In

[1] The research reported in this article has been supported by the Office of Naval Research, under contract Nonr. 2173(02).

order to allow the insertion of different sets of basic flux emissivity data into the heating rate calculations, the curve of flux emissivity versus optical thickness of water vapor was generated by fitting curves to the flux emissivity data rather than by the graphical method described by Brooks. Values of $\overline{\partial\epsilon(kw,T)/\partial w}$ over intervals of w were then computed from these analytical functions. In order to assess the error introduced into the results by this departure from Brooks' procedure, heating rates for a sample sounding were obtained both by a hand calculation using Brooks' method and from the computer program. The agreement between the two sets of values was very close, the average difference being only 0.07° C. day^{-1}.

2. INVESTIGATION OF BROOKS' METHOD

The case of a tropospheric temperature inversion was chosen as the means of investigating the effect of spacing of data points on heating rate profiles, the dependence of heating rates upon the flux emissivity data, and the influence of the form of the pressure correction factor upon heating rates. The soundings and heating rate profiles to be considered are presented in figures 1 to 3. For the sake of convenience and economy, calculations of heating rates were performed for each case at 10-mb. intervals of pressure. This pressure increment corresponds to a maximum water vapor thickness of 0.014 cm. in each layer of the lower levels and to a maximum water vapor optical thickness of 0.0003 cm. in each layer above the moisture decrease.

Figure 1 illustrates the situation of a rapid decrease of water vapor mixing ratio at a level just above the top of the 2° C. temperature inversion. The heating rate profile shows a maximum cooling rate of 6° C. day^{-1} just above the top of the inversion and a warming rate of 0.7° C. day^{-1} at the base. Thus, the combined effect of these two factors tends to destroy the inversion. In fact, if extrapolated, these heating rates will completely erode the inversion within 24 hr. In figure 2 the decrease of mixing ratio begins within the inversion. The heating rate profile, if extrapolated for a 24-hr. period, will leave the shape of the inversion essentially unchanged. Figure 3 represents the frequently observed situation in which an abrupt decrease of mixing ratio occurs a short distance below the base of the inversion. Maximum cooling occurs just below the base, while relative warming exists near the top. The heating rate profile now acts to intensify the inversion, and in a period of 24 hr. would double the magnitude of the inversion to 4° C.

In summarizing the above discussion, one can say that radiative heating tends to destroy a tropospheric temperature inversion if the air within the boundaries of the inversion is quite moist. However, as the relative humidity within the inversion is decreased, this effect becomes less pronounced. Finally, when moisture content decreases rapidly upward from the inversion base or from just below the base, as is frequently observed in the troposphere, radiative heating acts to maintain or even

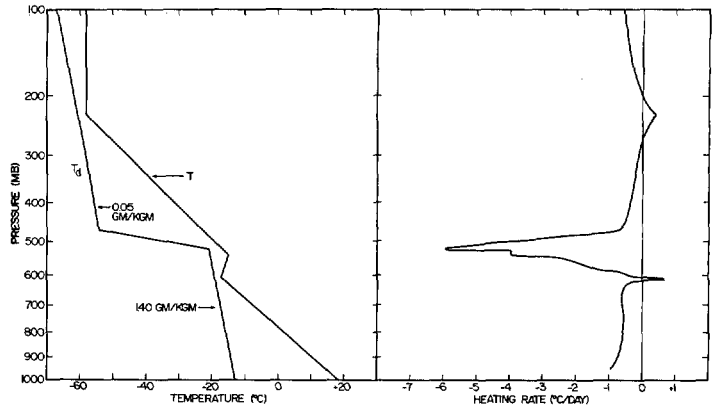

FIGURE 1.—Sounding 1 with radiative heating rate profile. Mixing ratio is indicated along segments of dew poin tcurve for which it is constant.

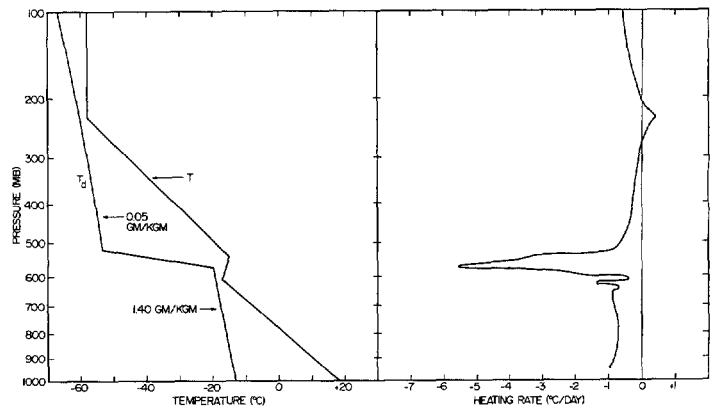

FIGURE 2.—Same as figure 1 for sounding 2.

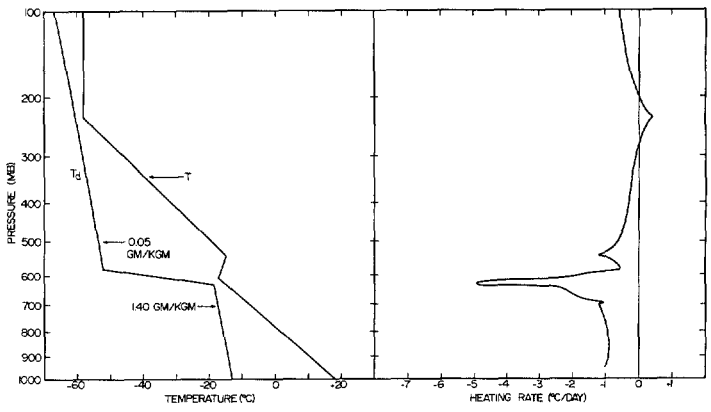

FIGURE 3.—Same as figure 1 for sounding 3.

to intensify the temperature inversion. Staley [13] arrived at the same conclusion based upon both theoretical calculations and measurements with the radiometersonde.

One problem which immediately confronts the person employing Brooks' method is that of choosing the number of levels at which to make calculations of radiative heating rates. The ordinary procedure when working with radiosonde data is to use all of the information available from a given flight. However, one cannot be positive that a

more accurate and detailed profile could not be obtained if a greater number of data points were available. Perhaps it would be wise to interpolate between the given values in order to obtain somewhat better estimates of the heating rates.

A brief investigation of this point has been made, the sounding of figure 3 being chosen for the sample calculations. When calculations were made using data points at 50-mb. intervals, many important features of the heating rate profile were lost. Both the cooling maximum and the cooling minimum between 500 and 600 mb. were completely absent. In addition, the magnitude of the cooling maximum between 600 and 650 mb. was reduced to one-half of its true value. As another test, the density of data points was increased in the most critical region of the sounding, near and within the temperature inversion. The calculations in this case led to a heating rate profile nearly identical to that of figure 3 for which data points were taken at every 10-mb. interval. Consequently, one concludes that any attempt to reduce the number of calculations by using data at widely spaced intervals will result in a heating rate profile quite different from the true one.

One factor which contributes directly to the reliability of radiative heating rate calculations by Brooks' method is the sensitivity of the method to the flux emissivity data. In order to estimate this dependence, new flux emissivity data presented by Zdunkowski and Johnson [16] have been used to make heating rate calculations with Brooks' method. A comparison between their values for a temperature of 20° C. and Brooks' original data is presented in table 1. The sample case chosen is the sounding of figure 3, with calculations made at 10-mb. intervals.

The results of this study are presented in figure 4. The solid line represents the heating rate profile obtained with Brooks' original flux emissivity data, and the dashed line represents calculations performed with Zdunkowski and Johnson's new values. The dominant feature of figure 4 is that the two profiles exhibit the same characteristics throughout the region of computations. Small differences, averaging 0.2° C. day^{-1}, which reach a maximum of 1° C. day^{-1} at 620 mb., do exist between the two profiles. Thus, one can state that Brooks' method displays a moderate sensitivity to the values of flux emissivity used as input parameters. However, it appears

TABLE 1.—*Emissivity data of Brooks [1] and of Zdunkowski and Johnson [16].*

Optical Depth (cm.)	Emissivity	
	Brooks	Zdunkowski & Johnson
0.00001	0.0029	0.0027
0.00010	0.0244	0.0247
0.00100	0.1155	0.1150
0.01000	0.2456	0.2890
0.10000	0.3959	0.4540
1.00000	0.5752	0.5950
5.00000	0.7020	0.7040

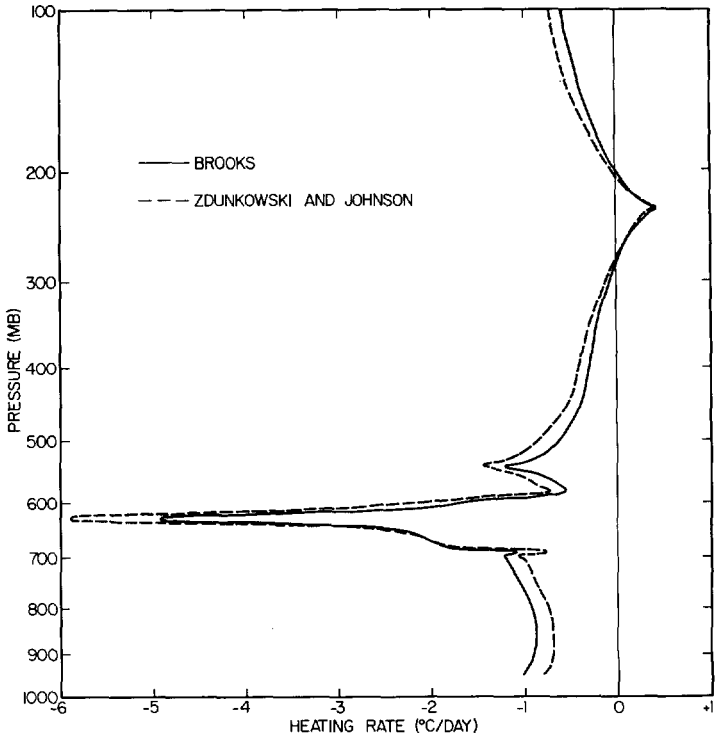

FIGURE 4.—Dependence of radiative heating rates upon the flux emissivity data. The temperature and mixing ratio data are from the sounding of figure 3.

that calculations based upon any reasonable set of values will yield results which, for all practical purposes, may be considered equal.

Another factor which directly influences the reliability of the results is the degree to which flux emissivity depends upon temperature. Elsasser and Culbertson [5] derived a theoretical relationship showing that emissivity is proportional to $T^{-\frac{1}{2}}$. Over the range of temperature in the atmosphere this dependence would produce only slight changes in the value of emissivity, and can, hence, be neglected. Brooks [1] based his method for calculating radiative heating rates upon the experimental data of F. A. Brooks [2] and of Robinson [12], who infers a slight increase in emissivity with temperature between 0° and 25° C. Brooks concluded that this dependence, which is opposite in sense to that derived by Elsasser, is not reliable and may be neglected. Goody [6] merely states that between 200° and 310° K. emissivity varies little with temperature.

Estimates of the influence which would be exerted upon radiative heating rates by temperature dependent flux emissivities have been obtained by assuming the inverse square-root dependence derived by Elsasser. Brooks' data were taken to apply at a temperature of 10° C., and from these values were generated data for 200°, 250°, and 300° K. These sets of values were substituted for Brooks' original data and heating rates were calculated for several cases. In no instance did the

TABLE 2.—*Rate of temperature change (°C. day $^{-1}$) given by methods of Brooks [1] and of Yamamoto and Onishi [15] for London's [8] model atmosphere, 0°–10° N., with clear skies*

Height (km.)	Brooks	Yamamoto & Onishi	Difference
0	−3.50	−2.20	1.30
1	−1.77	−1.73	0.04
2	−2.07	−1.64	0.43
4	−2.34	−1.87	0.47
6	−2.70	−2.29	0.41
8	−2.97	−2.29	0.68
10	−3.32	−2.29	1.03
12	−1.63	−1.74	−0.11
14	−0.61	−0.68	−0.07
16	−0.16	−0.14	0.02

different data alter the shape of the heating rate profile, although average differences up to 0.2° C. day^{-1} did appear in some instances.

A second indication of the effect of temperature variation of flux emissivities upon radiative heating rates can be found by comparing the results obtained for a particular case from Brooks' method and from another technique which allows for dependence of flux emissivities upon temperature. The method chosen was the radiation chart of Yamamoto and Onishi [15]. A comparison of results from these two methods for the data of London [8] in the latitude zone 0°–10° N. with clear skies in March is presented in table 2. The observed differences of several tenths of a °C. day $^{-1}$ are of the order of the inherent accuracy of these computational techniques. Of particular importance is the close agreement at upper levels, for this is the region of most interest in section 3 of this paper. On the basis of these findings, one feels justified in adopting the assumption made by Brooks that flux emissivity is independent of temperature. The complete solution of this problem requires spectrally resolved emissivity data for many path lengths and several temperatures within the atmospheric range over the entire wavelength range of importance, from 1 to 100 microns.

The concept of a pressure correction factor was introduced in equation (1). The manner in which pressure broadening is accounted for by correcting the water vapor optical thickness is explained in Elsasser's [4] original study. However, in that paper he incorrectly concluded that pressure broadening may be treated by correcting the optical thickness of water vapor by a factor $(p/p_s)^{1/2}$, where p is the mean pressure of the layer and p_s is a standard value, usually taken as 1000 mb. In a later work, Elsasser and Culbertson [5], this error was corrected, and the theoretical pressure correction factor was properly given as $(p/p_s)^{1.0}$. It should be pointed out that the above results depend upon the assumption that individual absorption lines take on the Lorentz line shape. In experimental work with specific absorption bands, where this assumption does not hold, different correction factors, such as $(p/p_s)^n$ where n lies between 0.5 and 1.0, have been obtained from various curve-fitting techniques.

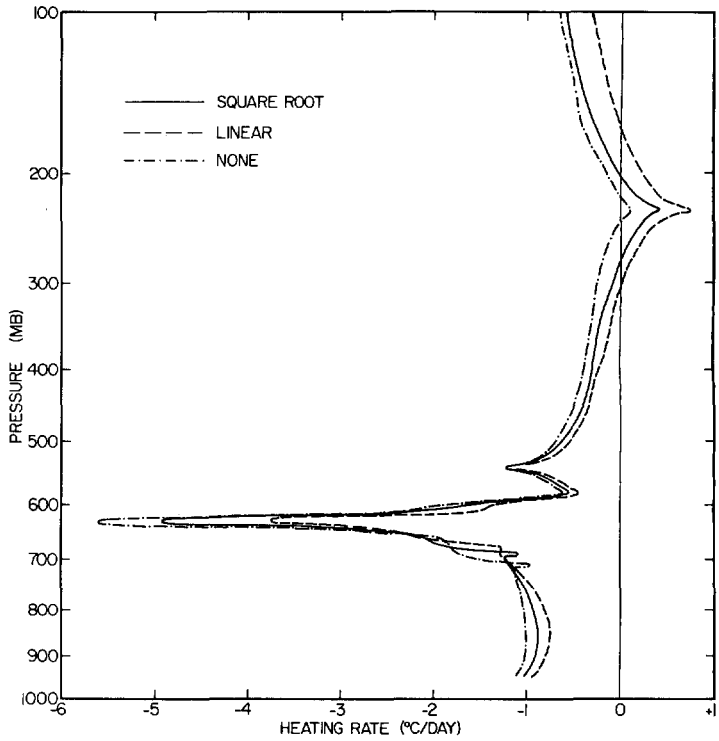

FIGURE 5.—Effect of the pressure correction factor $(p/p_s)^n$ on heating rate profiles. The three cases considered are $n=1/2$, square root pressure correction; $n=1$, linear pressure correction; $n=0$, no pressure correction. The temperature and mixing ratio data are from the sounding of figure 3.

It is apparent from the above statements that many different forms of the pressure correction factor have been available for radiative heating rate calculations. Most of the earlier studies followed Elsasser's first paper and used $(p/p_s)^{1/2}$; this was the form chosen by Brooks for his method. As experimental investigation of the important absorption bands became possible, various values for n between 0.5 and 1.0 were proposed. In some studies, Staley [13], the pressure correction factor has been neglected entirely because of the uncertainty of its form.

In an attempt to estimate the dependence of the calculated heating rate values upon the pressure correction factor $(p/p_s)^n$, three different forms were used to correct optical thickness in computing heating rates for a sample atmospheric sounding. The cases chosen were square-root pressure correction, linear pressure correction, and no pressure correction. As before, the atmospheric state chosen was the sounding of figure 3. The results of this study are presented in figure 5. It is seen that, although the basic features of the heating rate profile have not been altered by the form of the presssure correction factor, significant differences of the order of several tenths of a °C. day $^{-1}$ do exist among the heating rates in the different profiles. Therefore, it is suggested that the theoretically correct linear pressure correction factor be used in order to obtain maximum accuracy.

3. APPLICATION OF BROOKS' METHOD

The problem which has been chosen to provide an illustration of the usefulness of the computer program in lengthy calculations is that of evaluating heating rates over a cross section of the Northern Hemisphere. It was decided to test the consequences of the two possible cases of a dry stratosphere and of a moist stratosphere. The monthly mean aerological cross sections published by the U.S. Weather Bureau [14] for the period of the International Geophysical Year (IGY) were chosen as the source of tropospheric data. The cross section used as a basis for the heating rate calculations is that for January 1958.

Heating rates were calculated for two atmospheric states over the Northern Hemisphere. In both cases the mixing ratio profiles matched those of the IGY data as high as such values were given. For the dry stratosphere case, the water vapor content was then allowed to decrease at a uniform rate, approaching zero near the 10-mb. level. In order to treat the case of a moist stratosphere, it was decided that a reasonable upper limit for stratospheric water vapor content could be represented by a relative humidity of 5 percent. The water vapor content was therefore allowed to decrease at a uniform rate above the IGY data until a state of 5 percent relative humidity was reached. The mixing ratio profiles were then continued upward always maintaining this value. The cross sections depicting typical winter conditions over the Northern Hemisphere with a dry stratosphere and with a constant 5 percent relative humidity stratosphere are presented in figures 6 and 7, respectively.

Several features of the temperature fields, identical in both cases, can be distinguished. In high latitudes above the tropopause, located near the 250-mb. level, temperatures decrease with height at a slower rate than in the troposphere. In middle latitudes a nearly isothermal condition exists above the tropopause, located at approximately 250 mb. In low latitudes temperatures increase sharply above the tropopause which is located near the 100-mb. level.

The mixing ratio fields are identical from the surface up to the level at which a relative humidity of 5 percent is attained. This level is located throughout the cross section at approximately the level of the tropopause. Above the tropopause the mixing ratio fields are very different. In figure 6 mixing ratios continue to decrease with height up to the 10-mb. level. However, in figure 7 a 5 percent relative humidity is maintained throughout the stratosphere. In high latitudes the effects of slowly decreasing temperature and decreasing pressure offset each other, and mixing ratios remain nearly constant above the tropopause. In middle latitudes where temperatures remain nearly constant above the tropopause, the mixing ratios increase slowly as pressure decreases to 10 mb. In low latitudes, as temperatures increase sharply above the tropopause, mixing ratios also increase rapidly with height.

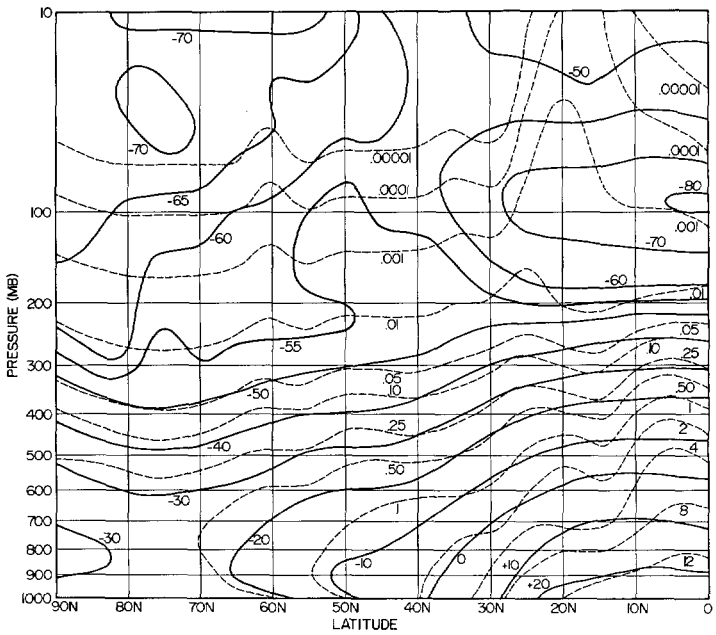

FIGURE 6.—Temperature and mixing ratio fields for Northern Hemisphere cross section with dry stratosphere. Solid lines are isotherms (° C.) and dashed lines are mixing ratios (gm. kgm.$^{-1}$).

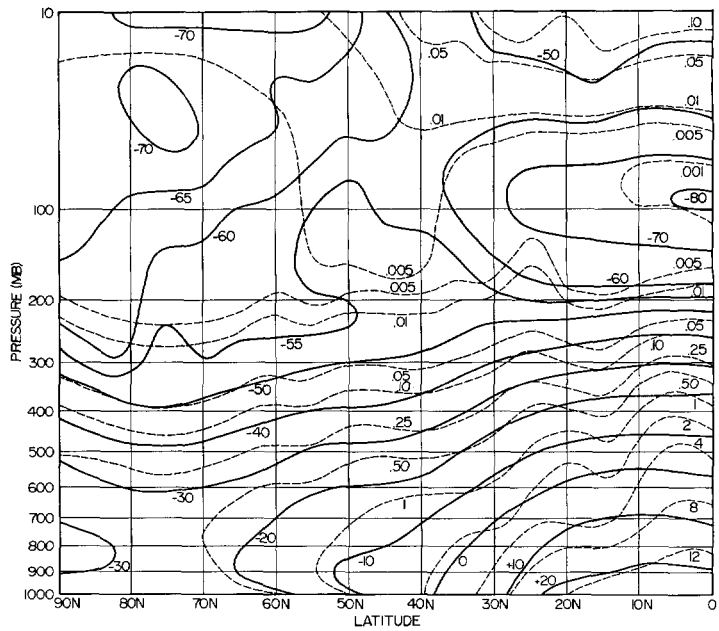

FIGURE 7.—Temperature and mixing ratio fields for Northern Hemisphere cross section with constant 5 percent relative humidity stratosphere. Solid lines are isotherms (° C.) and dashed lines are mixing ratios (gm. kgm. $^{-1}$).

Temperature, pressure, and mixing ratio data were obtained from figures 6 and 7 from the equator to the pole at intervals of 5° of latitude. These data were then employed to form an atmospheric sounding at each location, and the heating rate profiles were computed using Brooks' method. Heating rates were calculated at 10-mb. intervals of pressure between 1000 and 100 mb., at 5-mb.

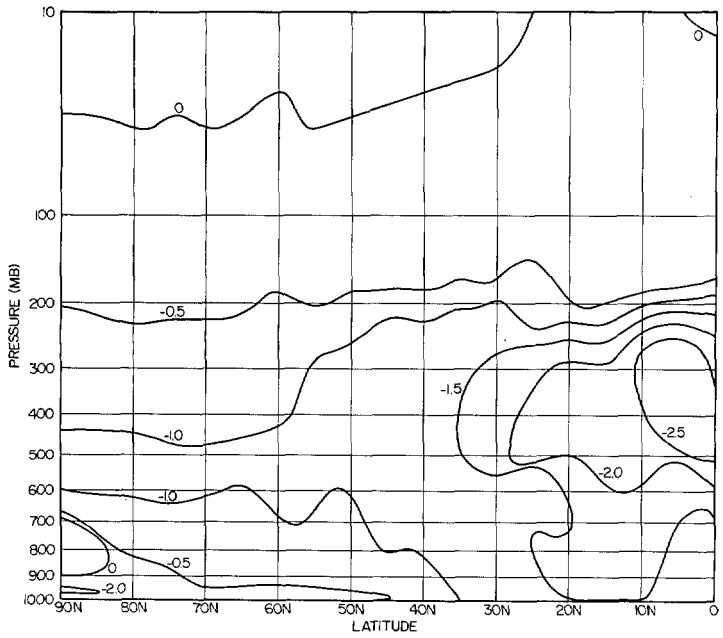

FIGURE 8.—Heating rate cross section for Northern Hemisphere with dry stratosphere. Heating rates are given in units of ° C. day^{-1}.

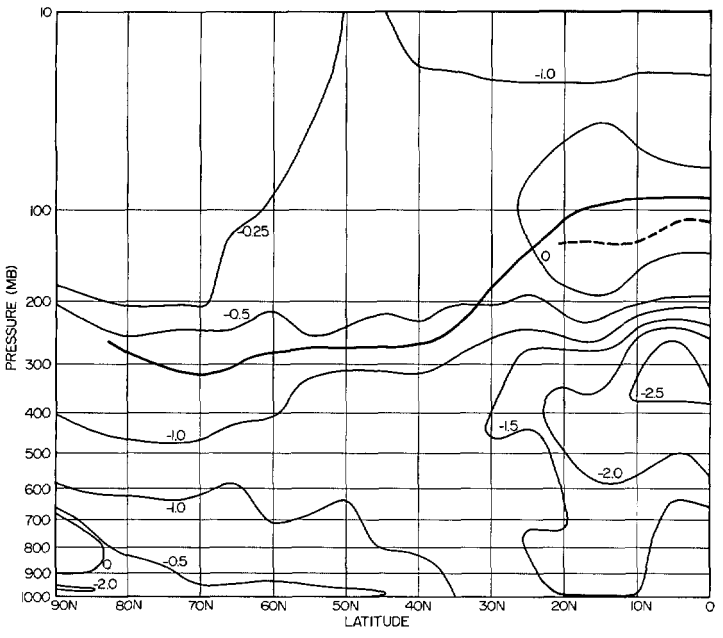

FIGURE 9.—Heating rate cross section for Northern Hemisphere with constant 5 percent relative humidity stratosphere. Heating rates are given in units of ° C. day^{-1}. The heavy solid line indicates the location of the tropopause; the heavy dashed line the location of heating rate maxima in the region from the equator to 20° N.

intervals between 100 and 30 mb., and at 2-mb. intervals between 30 and 10 mb. With this choice of pressure increments, the optical thickness of water vapor in a single layer exceeds 0.01 cm. only in the lower levels of the moist regions, below the 1-gm. kgm.$^{-1}$ mixing ratio line in figures 6 and 7. The results were compiled to form cross sections of the Northern Hemisphere, presented in figures 8 and 9 for the cases of the dry and moist stratosphere, respectively.

The outstanding feature of figure 8 is the center of maximum radiative cooling located in tropical latitudes near the 400-mb. level. The existence of this phenomenon may be explained in the following manner. The net upward flux at any level is the difference between the energy arriving from radiating layers below and the energy arriving from the radiating layers above. If this difference increases with height, the net upward flux also increases with height. Thus, the layers are transporting more heat upward than they are receiving, and will cool. This situation exists between the surface and 400 mb. in tropical latitudes, the increase in net upward flux being attributed to the rapid decrease of water vapor content from the high surface values of mixing ratio over tropical regions. Above the 400-mb. level, the effect of increasing temperatures above the tropopause begins to be felt, and cooling rates decrease. In the upper levels mixing ratios decrease to such low values that very little water vapor is available for the absorption and reradiation of energy. Consequently, radiative cooling rates approach zero. Over the rest of the cross section the same behavior is observed to a lesser degree. Cooling rates increase with height from the surface up to approximately the 500-mb. level, and then decrease toward zero as the water vapor content approaches zero.

In figure 9 the presence of appreciable quantities of water vapor in the stratosphere produces a quite different radiative heating rate cross section. However, to be pointed out first is the similarity between figures 8 and 9 in the lower levels. This, of course, is because the temperature and mixing ratio fields are identical from the surface up to approximately the tropopause. The slight differences which do occur may be attributed to the influence felt in lower levels of water vapor absorption and reradiation in the stratosphere.

The location of the tropopause has been indicated by a heavy solid line in figure 9 for the purpose of the following discussion. In high latitudes the presence of slightly greater quantities of water vapor in the stratosphere than were present in the previous case produces greater radiative energy transfer from these levels. Consequently, the cooling rates approach zero more slowly than they did in figure 8. In middle latitudes the mixing ratios increase slowly with height above the tropopause. This increase is sufficient to maintain a nearly constant cooling rate of approximately 0.5° C. day^{-1} in the stratosphere. The rapid increase of water vapor content above the tropopause in low latitudes has a very striking effect. The increased radiative transfer of energy from this region produces an increased downward flux. This effect is so pronounced in the neighborhood of the 100-mb. level that

the net upward flux actually decreases slightly with height. The result, as seen in figure 9, is that there is a tendency for the region to be warmed radiatively. The levels of maximum radiative warming from the equator to 20° N. have been indicated by a heavy dashed line. The maximum value reached is 0.07° C. day^{-1} at 15° N.

The decrease of net radiative flux was observed by Riehl [11] while making measurements in the Caribbean with the Suomi-Kuhn infrared radiometer. A mean sounding of 116 ascents at five stations revealed a decrease from near 200 mb. to the vicinity of the tropopause, located between 80 and 100 mb. This layer of decreasing flux was present on nearly all of the individual soundings, and calculations of heating rates led to warming in the layer from 100 to 200 mb. Similar results were obtained by Kuhn and Suomi [7] while analyzing radiometersonde flux measurements from 15 ascents over the United States. Warming trends were observed in the region from 100 to 200 mb. in the vicinity of the tropopause.

A second feature present in both of these investigations is exhibited in figure 9. The level of maximum warming was observed approximately 50 mb. below the tropopause by Riehl. Kuhn and Suomi found the level of maximum warming to occur from 25 to 50 mb. below the level of the tropopause. Investigation of figure 9 also shows that the level of maximum warming, indicated by the heavy dashed line, is located from 25 to 50 mb. below the tropopause. Since temperatures both above and below the tropopause are greater than at the level of minimum temperature, one might expect maximum warming to take place at the tropopause. However, the vertical distribution of water vapor in this region plays an important role in determining the radiative heating rates. We have already pointed out that the presence of substantial quantities of water vapor above the tropopause produces an increased downward flux of energy from these levels. Since mixing ratios in the immediate vicinity of the tropopause are very low, only small amounts of this energy are absorbed at the tropopause. The greater portion of the energy passes through this region and is absorbed at lower levels where substantial quantities of water vapor are present. The absorption of energy at these levels is reflected by the presence of maximum warming rates 25 to 50 mb. below the tropopause.

In summary, one may state that the results of this study lend support to the argument that substantial quantities of water vapor do exist in the stratosphere. When the assumption was made that the water vapor content decreased to zero above the tropopause, the computed cooling rates were also observed to decrease toward zero in the stratosphere. However, when the assumption was made that relative humidities of 5 percent exist in the stratosphere, the computed cooling rates agreed very well with the observed phenomenon of radiative warming in the neighborhood of the tropopause at low latitudes. Further, the location of the levels of maximum warming from 25 to 50 mb. below the tropopause was observed both in this study and in the experimental measurements.

ACKNOWLEDGMENTS

The author wishes to express his special appreciation to Dr. Dean O. Staley for his assistance and guidance in the preparation of this paper. Gratitude is also extended to Dr. Benjamin M. Herman for his helpful discussions on atmospheric radiation processes.

REFERENCES

1. D. L. Brooks, "A Tabular Method for the Computation of Temperature Change by Infrared Radiation in the Free Atmosphere," *Journal of Meteorology*, vol. 7, No. 5, Oct. 1950, pp. 313–321.
2. F. A. Brooks, "Observations of Atmospheric Radiation," *Papers in Physical Oceanography and Meteorology*, Massachusetts Institute of Technology and Woods Hole Oceanographic Institution, vol. 8, No. 2, Oct. 1941, 23 pp.
3. A. Bruinenberg, "Een Numerieke Methode voor de Bepaling van Temperatuurs-Veranderingen door Straling in de Vrije Atmosfeer," (A Numerical Method for the Calculation of Temperature Changes by Radiation in the Free Atmosphere), Köninlijk Nederlands Meteorologisch Instituut, No. 125, *Mededelingen en Verhandelingen*, Series B, vol. 1, No. 1, 1946, 52 pp.
4. W. M. Elsasser, "Heat Transfer by Infrared Radiation in the Atmosphere," *Harvard Meteorological Studies*, No. 6, Harvard University Press, Cambridge, 1942, 107 pp.
5. W. M. Elsasser with M. F. Culbertson, "Atmospheric Radiation Tables," *Meteorological Monographs*, vol. 4, No. 23, American Meteorological Society, Boston, Aug. 1960, 43 pp.
6. R. M. Goody, *Atmospheric Radiation, Vol. I, Theoretical Basis*, Clarendon Press, Oxford, 1964, 436 pp.
7. P. M. Kuhn and V. E. Suomi, "Infrared Radiometer Soundings on a Synoptic Scale," *Journal of Geophysical Research*, vol. 65, No. 11, Nov. 1960, pp. 3669–3677.
8. J. London, "The Distribution of Radiational Temperature Change in the Northern Hemisphere during March," *Journal of Meteorology*, vol. 9, No. 2, Apr. 1952, pp. 145–151.
9. F. Möller, *Das Strahlungsdiagram*, Reichsampt für Wetterdienst, Berlin, 1943, 9 pp.
10. R. Mügge and F. Möller, "Zur Berechnung von Strahlungsströmen und Temperaturänderungen in Atmosphären von Beliebigen Aufbau," *Zeitschrift für Geophysik*, vol. 8, Nos. 1–2, 1932, pp. 53–64.
11. H. Riehl, "Radiation Measurements Over the Caribbean During the Autumn of 1960," *Journal of Geophysical Research*, vol. 67, No. 10, Sept. 1962, pp. 3935–3942.
12. G. D. Robinson, "Notes on the Measurement and Estimation of Atmospheric Radiation—2," *Quarterly Journal of the Royal Meteorological Society*, vol. 76, No. 327, Jan. 1950, pp. 37–51.
13. D. O. Staley, "Radiative Cooling in the Vicinity of Inversions and the Tropopause," *Quarterly Journal of the Royal Meteorological Society*, vol. 91, No. 389, July 1965, pp. 282–301.
14. U.S. Weather Bureau, *Monthly Mean Aerological Cross Sections Pole to Pole Along Meridian 75° W. for the IGY Period*, Washington, D.C., 1961.
15. G. Yamamoto and G. Onishi, "A Chart for the Calculation of Radiative Temperature Changes," *Science Reports*, Tohoku University, 5th Series, Geophysics, vol. 4, No. 3, Mar. 1953, pp. 108–115.
16. W. G. Zdunkowski and F. G. Johnson, "Infrared Flux Divergence Calculations With Newly Constructed Radiation Tables," *Journal of Applied Meteorology*, vol. 4, No. 3, June 1965, pp. 371–377.

[*Received January 17, 1966; revised June 29, 1966*]